



Research Paper

Mafic Archean continental crust prohibited exhumation of orogenic UHP eclogite

Richard M. Palin^{a,*}, James D.P. Moore^{b,c}, Zeming Zhang^d, Guangyu Huang^e, Jon Wade^a, Brendan Dyck^f^a Department of Earth Sciences, University of Oxford, Oxford OX1 3AN, United Kingdom^b Earth Observatory of Singapore, Nanyang Technological University, Singapore^c Institute of Geophysics, SGEES, Victoria University of Wellington, Wellington, New Zealand^d Institute of Geology, Chinese Academy of Geological Sciences, Beijing 100037, China^e State Key Laboratory of Lithospheric Evolution, Institute of Geology and Geophysics, Chinese Academy of Sciences, Beijing 100029, China^f Department of Earth, Environmental and Geographical Sciences, University of British Columbia, Kelowna V1V 1V7, Canada

ARTICLE INFO

Article history:

Received 30 March 2021

Revised 29 April 2021

Accepted 7 May 2021

Available online 9 May 2021

Handling Editor: M. Santosh

Keywords:

Archean

Eclogite

Exhumation

Secular change

Geodynamics

Density

ABSTRACT

The absence of ultrahigh pressure (UHP) orogenic eclogite in the geological record older than c. 0.6 Ga is problematic for evidence of subduction having begun on Earth during the Archean (4.0–2.5 Ga). Many eclogites in Phanerozoic and Proterozoic terranes occur as mafic boudins encased within low-density felsic crust, which provides positive buoyancy during subduction; however, recent geochemical proxy analysis shows that Archean continental crust was more mafic than previously thought, having greater proportions of basalt and komatiite than modern-day continents. Here, we show via petrological modelling that secular change in the petrology and bulk composition of upper continental crust would make Archean continental terranes negatively buoyant in the mantle before reaching UHP conditions. Subducted or delaminated Archean continental crust passes a point of no return during metamorphism in the mantle prior to the stabilization of coesite, while Proterozoic and Phanerozoic terranes remain positively buoyant at these depths. UHP orogenic eclogite may thus readily have formed on the Archean Earth, but could not have been exhumed, weakening arguments for a Neoproterozoic onset of subduction and plate tectonics. Further, isostatic balance calculations for more mafic Archean continents indicate that the early Earth was covered by a global ocean over 1 km deep, corroborating independent isotopic evidence for large-scale emergence of the continents no earlier than c. 3 Ga. Our findings thus weaken arguments that early life on Earth likely emerged in shallow subaerial ponds, and instead support hypotheses involving development at hydrothermal vents in the deep ocean.

© 2021 China University of Geosciences (Beijing) and Peking University. Production and hosting by Elsevier B.V. This is an open access article under the CC BY-NC-ND license (<http://creativecommons.org/licenses/by-nc-nd/4.0/>).

1. Introduction

Eclogites are high-pressure (HP) metabasic rocks dominated by garnet and omphacite (Haüy, 1822), and typically occur as xenoliths in mantle-derived magmas, boudins/lenses within felsic gneiss terranes, blocks encased within tectonic mélange, or metamorphosed and exhumed slices of oceanic lithosphere (Coleman et al., 1965). A subdivision of the eclogite facies is defined by pressure–temperature (*P*–*T*) conditions sufficient to transform quartz to coesite (~2.6–2.8 GPa at ~500–900 °C), which is termed ultrahigh pressure (UHP) metamorphism (Hacker, 2006). At lithostatic pressures, this is achieved at depths of ~90–100 km below the Earth's surface (Hernández-Urbe and Palin, 2019).

Geodynamic calculations show that mafic oceanic crust transported into the mantle at convergent plate margins cannot be exhumed by buoyancy alone after reaching ~50–60 km (*P* = 1.4–1.8 GPa) (Agard et al., 2009), although felsic continental crust remains positively buoyant to much greater depths (85–160 km; *P* = 2.6–5 GPa) (Chapman et al., 2019). These results corroborate observations from the rock record that most UHP basic eclogite occurs in orogenic geological settings (Hacker, 2006; Liou et al., 2009), where dismembered meta-mafic pods are encased within high-temperature/low-pressure felsic orthogneiss (St-Onge et al., 2013). These mafic components represent dikes or sills intruded into the shallow levels of continental crust prior to collisional orogeny, with the leading edge of the continental margin thinned, subducted, metamorphosed, and exhumed (Gilotti, 2013). Exhumation of this upper crust may occur via wholesale slab breakoff (i.e. detachment from the preceding oceanic lithosphere)

* Corresponding author.

E-mail address: richard.palin@earth.ox.ac.uk (R.M. Palin).

or else separation from the middle to lower continental crust, which may continue to descend into the mantle (e.g. Warren, 2013). By contrast, non-orogenic eclogite types represent fragments of exhumed oceanic crust that are not genetically associated with continental crustal materials, such that their mechanisms of exhumation are more uncertain.

The oldest UHP continental eclogite on Earth (c. 630 Ma) occurs in the Pan African orogenic belt, Southwestern Brazil (Liou et al., 2009). Additionally, the oldest continental (orogenic) HP eclogite (c. 2.09 Ga) is located in Cameroon and formed during the Eburnian collisional orogeny (Loose and Schenk, 2018). These occurrences support the low density of felsic continental crust being a critical factor that allows exhumation of these subducted terranes back to the Earth's surface (Boutelier et al., 2004). Given multiple independent lines of evidence for subduction and collisional orogenesis having operated on Earth since at least the middle Archean (c. 3 Ga; Palin et al., 2020), the absence of (U)HP eclogite in the rock record older than c. 2 Ga is unexpected.

In this study, we test the petrophysical implications of recent geochemical proxy analysis showing that juvenile continental crust on the early Earth was significantly more mafic than previously thought (Tang et al., 2016; Chen et al., 2020). Thermodynamic phase equilibrium modelling of reconstructed bulk compositions for Archean, Proterozoic, and Phanerozoic upper continental crust (UCC) and continental basalt shows that the 'point of no return' for slivers of Archean continents transported to mantle depths is reached before the HP–UHP transition. By contrast, more silica-rich Phanerozoic and Proterozoic UCC remains positively buoyant to much greater depths, and so may be readily exhumed. This secular change in density contrast is independent of hydration state and implies that UHP rocks likely formed on the early Earth by transport of crustal materials to mantle depths, yet could not be returned to the surface via buoyancy alone.

2. Models of secular change in continental crust composition

Early studies of continental crust composition using surface sampling, weighted compositions of stratigraphic successions, and/or crustal xenoliths produced conflicting interpretations due to the different levels of exposure and tectonic histories of each studied region (Holland and Lambert, 1972; Taylor and McLennan, 1995). In response, Condie (1993) combined geochemical analyses with isotopic data to consider only juvenile lithological components and interpreted that the UCC has remained dacitic in bulk composition ($\text{SiO}_2 = 65\text{--}67\text{ wt\%}$) since c. 3.5 Ga (Fig. 1). However, recently, various geochemical proxies infer that the maficity ($\text{FeO} + \text{MgO}$) of UCC has shown greater change through time. Greber et al. (2017) used changing Ti isotope and Ni/Co ratios of terrigenous sediments to suggest that Archean UCC had a relatively lower (andesitic) bulk SiO_2 content of ~62 wt% (Fig. 1). By contrast, Chen et al. (2020) used Cu/Ag ratios in glacial diamictites to show that the UCC contained significant volumes of mafic and ultramafic components at c. 3.0 Ga, and transitioned to a felsic-rock-dominated crust at c. 2.4 Ga, with minimal change since (Fig. 1, Table 1). These latter findings match calculated Rb/Sr ratios of juvenile volcanic and plutonic igneous rocks showing that the pre-3 Ga bulk continental crust was mafic in composition (~50 wt% SiO_2), and evolved to felsic values (~58 wt% SiO_2) during the Proterozoic (Dhuime et al., 2015). This change is also consistent with c. 3.7–3.8 Ga immature clastic metasediments from the Eoarchean Isua complex, west Greenland, that have mafic compositions (Bolhar et al., 2005), implying a SiO_2 -poor UCC (Fig. 2).

Here, we undertook modelling to quantify the petrophysical implications of these interpretations that Archean UCC was more mafic than previously thought, which involved determining

mineral assemblages and bulk densities for UCC lithologies in orogenic terranes that may be transported to mantle depths via subduction. As fluid content can control reaction progress during metamorphism, we considered both nominally anhydrous (NAN) and minimally hydrated (MHy) conditions, which represent end-members of a spectrum of fluid contents documented in nature (Deming, 1994). Calculations were also performed for anhydrous mantle pyrolite, and the density contrast between each lithology at any given P – T condition was used to determine whether buoyancy-driven exhumation was possible (Weller et al., 2019), assuming the crustal components could mechanically detach from the descending lithosphere.

Secular variation was initially modelled using the reconstructed lithological proportions for Archean (3 Ga), Paleoproterozoic (2.4 Ga), and Phanerozoic (0.3 Ga) UCC from Chen et al. (2020). Average compositions for greenstone/continental basalt of the same ages (Condie et al., 2016) were considered as mafic intrusions into these continental terranes, thus representing a precursor condition for generating orogenic eclogites. We chose the Archean UCC composition from Chen et al. (2020) defined by komatiite–basalt–felsic rock proportions of 20:69:11, which produces a SiO_2 content of ~51 wt% matching independently calculated compositions of juvenile continental crust at that time (~50 wt%; Dhuime et al., 2015). We subsequently applied the Monte Carlo analysis technique of Palin et al. (2016) to determine the sensitivity of our results with respect to uncertainty in lithological components reported by Chen et al. (2020) for UCC through time (see below).

Schematic profiles through each continental crust are presented in Fig. 2, with the UCC representing the top third of each column (Rudnick and Gao, 2003). While the composition of UCC is not necessarily equivalent to the entire continental crust, we focused on this uppermost domain for two reasons. First, analogue (e.g. Bialas et al., 2011) and numerical (e.g. Palin et al., 2017) modelling shows that it is UCC that is thinned and stretched at the leading edge of a terrane margin during continental subduction, and so is carried to eclogite-facies conditions. Second, in the case of wholesale continental subduction, it is the uppermost surface of the slab that will be preferentially weakened and detached due to deformation and fluid–rock interactions at the plate interface (Zheng et al., 2013).

3. Methods

3.1. Petrological modelling

Petrological modelling used to investigate the metamorphic phase transformations and density variations in all rock types was performed using the Gibbs free energy minimization program Theriak-Domino (De Capitani and Petrakakis, 2010) and the internally consistent thermodynamic dataset ds-62 (Holland and Powell, 2011). Phase equilibria for pyrolite (Ringwood, 1975) were calculated in the Na_2O – CaO – FeO – MgO – Al_2O_3 – SiO_2 – O_2 – Cr_2O_3 (NCFMASOcr) system using activity–composition (a – X) relations for olivine, garnet, clinopyroxene, orthopyroxene, spinel, plagioclase, and ultramafic silicate melt (Jennings and Holland, 2015). Phase equilibria for all crustal materials were calculated in the Na_2O – CaO – K_2O – FeO – MgO – Al_2O_3 – SiO_2 – H_2O – TiO_2 – O_2 (NCKFMASHTO) system using a – X relations for: clinopyroxene (diopside–omphacite–jadeite) and clinoamphibole (glaucophane–actinolite–hornblende) (Green et al., 2016); garnet, biotite, chloritoid, muscovite–paragonite, and chlorite (White et al., 2014); epidote (Holland and Powell, 2011); plagioclase (Holland and Powell, 2003); and ilmenite (White et al., 2000). Pure phases included aqueous fluid (H_2O) talc, lawsonite, kyanite, quartz, rutile, titanite, and albite.

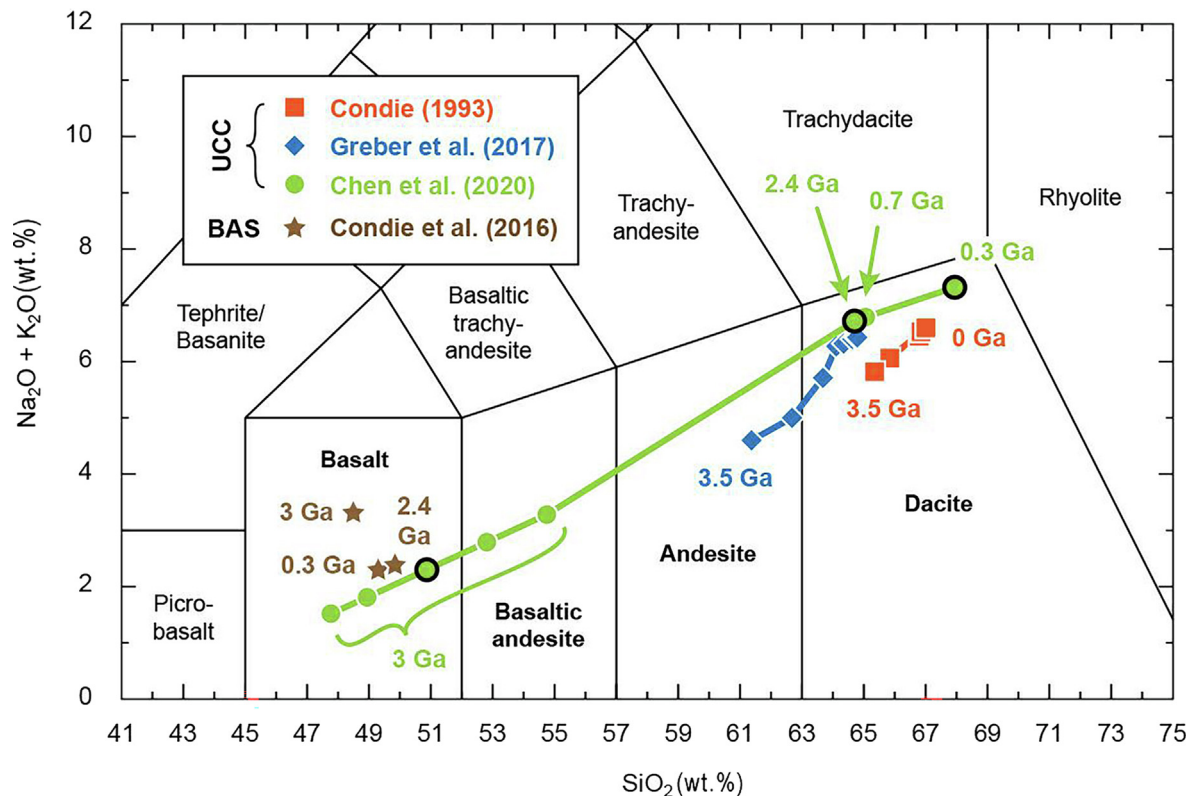


Fig. 1. Total alkali-silica diagram showing bulk compositions of crustal lithologies considered in this study. Representative compositions are shown for upper continental crust (UCC) and continental basalt (BAS) of Archean (3 Ga), Proterozoic (2.4 Ga), and Phanerozoic (0.3 Ga) age. Data are from [Condie \(1993\)](#), [Condie et al. \(2016\)](#), [Greber et al. \(2017\)](#), and [Chen et al. \(2020\)](#).

Table 1
Upper continental crust (UCC) compositions (weight % oxide) reconstructed by [Chen et al. \(2020\)](#), reported on an anhydrous basis with all iron as Fe²⁺. The Archean UCC composition considered here is for a komatiite-basalt-felsic rock ratio of 20:69:11. Interpreted juvenile continental crust thickness is from [Dhuime et al. \(2015\)](#). The UCC is taken to represent the top third of the entire crustal column.

Age (Ga)	Thickness (km)	SiO ₂	TiO ₂	Al ₂ O ₃	FeO ^{tot}	MnO	MgO	CaO	Na ₂ O	K ₂ O	P ₂ O ₅
Archean (3)	18	50.87	0.69	12.19	11.47	0.18	11.14	8.14	1.86	0.44	0.07
Paleoproterozoic (2.4)	25	64.70	0.69	14.84	5.33	0.08	2.26	3.86	3.48	3.24	0.17
Phanerozoic (0.3)	32	67.94	0.50	14.66	4.04	0.07	1.34	2.70	3.59	3.72	0.14

Two end-member hydration states were used for each crustal lithology: nominally anhydrous (NAn) and minimally hydrated (MHy). The former considered 1 mol.% H₂O within the bulk-rock composition, after [Wade et al. \(2017\)](#), and the latter considered a lithology-specific fluid content that allowed minimal free H₂O within the equilibrium phase assemblage during subduction. For mafic lithologies, this was ~10–13 mol.% (Table S1), which is comparable to measured H₂O contents in modern-day hydrated oceanic crust ([Staudigel, 2003](#)). A bulk-rock Fe³⁺/Fe^{total} ratio of 0.1 was applied to all rock types based on [Stagno et al. \(2013\)](#) and [Le Losq et al. \(2019\)](#); however, variation within the bounds of accepted uncertainty is unlikely to have any significant effect on calculated phase equilibria and/or petrophysical properties (cf. [Forshaw et al., 2019](#)). Calculations were performed using pressure-temperature (*P-T*) conditions defined for the slab surface of subducted crust in an ‘average’ subduction zone ([Penniston-Dorland et al., 2015](#)), which was defined from a compilation of exhumed (U)HP blueschist- and eclogite-facies rocks in Phanerozoic and Proterozoic terranes. This geotherm, however, is comparable to that purported for the late Archean based on geochemical modeling of tonalite-trondhjemite-granodiorite magma petrogenesis ([Martin and Moyen, 2002](#)), so is considered here for subducted crusts of all ages to allow direct comparison of density profiles. Finally, it is well understood that the Earth’s mantle has cooled

over geological time ([Herzberg et al., 2010](#)), which has led to some authors suggesting that subduction zones in the Archean would have had notably hotter slab-surface geotherms that seen in Phanerozoic equivalents. However, elevated mantle potential temperatures do not directly imply hotter slab surfaces along the subduction interface (see discussion in [Palin and White, 2016](#)) with the main controls on subduction zone thermal structure being convergence rate and slab age (e.g., [Kirby et al., 1991](#)). In a recent review of secular change in tectonics, [Korenaga \(2013\)](#) suggested that neither the tempo nor the average age of oceanic crust that was subducted in the Archean differed significantly from the present day; thus, we have chosen to fix a typical subduction zone geotherm for all instances. It is also noted that examples of Proterozoic HP eclogites (c. 2.1–1.8 Ga) often record prograde and peak *P-T* conditions that match those of Phanerozoic eclogites (e.g. [Weller and St-Onge, 2017](#)), supporting this simplification.

Sensitivity analysis of the uncertainty on UCC density and metamorphosed petrological constitution based on uncertainty in pre-subduction lithological proportions for Archean terranes was performed as outlined in the [Supplementary Data](#). This analysis demonstrates that the ‘depth of no return’ for most plausible iterations of subducted Archean UCC occurs consistently (~90% of all randomized bulk compositions) before the HP-UHP transition is reached.

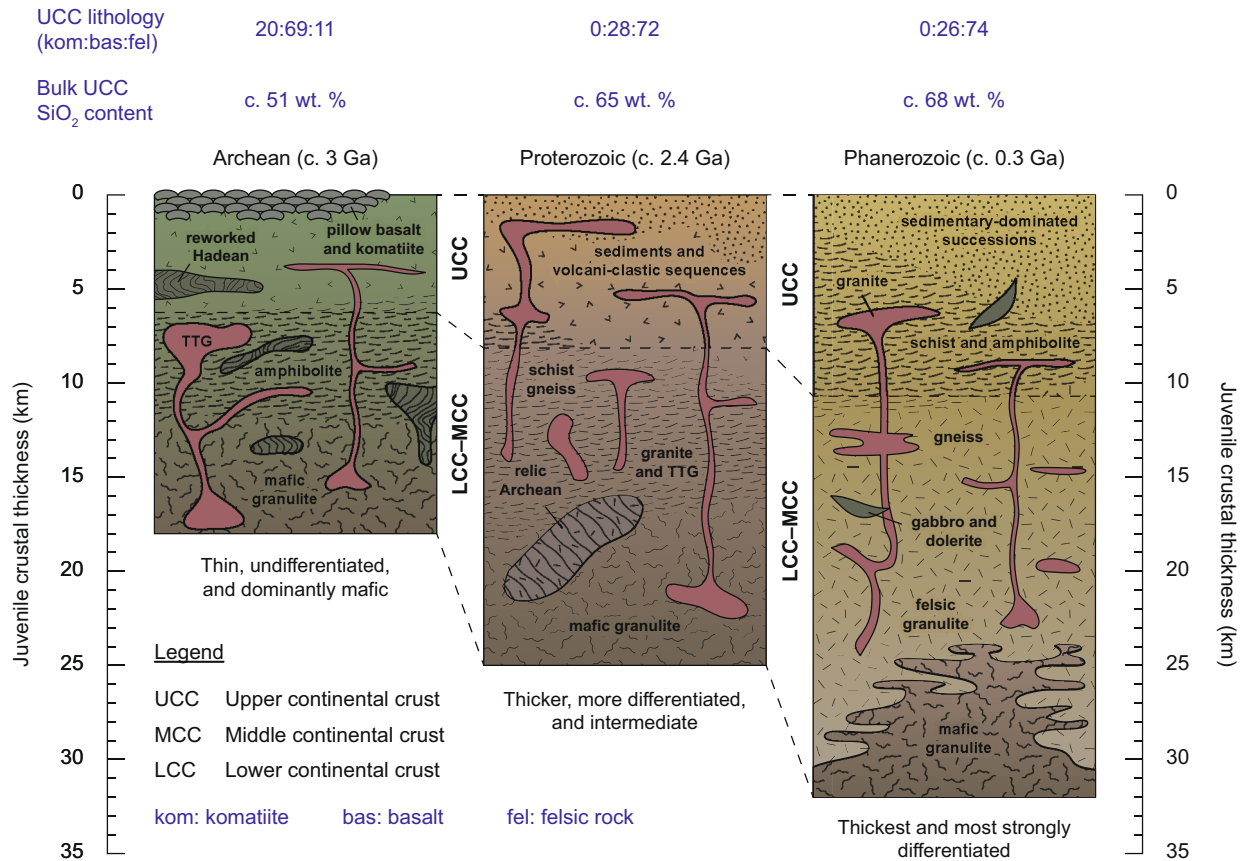


Fig. 2. Secular change in continental crust structure, lithology, and composition through time. Secular changes in reconstructed composition, thickness, and petrological components are emphasised. Phanerozoic and Proterozoic profiles modified after Hawkesworth et al. (2016).

3.2. Lithospheric strength modelling

We calculate yield strength envelopes (Watts, 2001) where failure is assumed to occur either by brittle deformation, governed by Byerlee's friction coefficients (Byerlee, 1978), or ductile flow (Kohlstedt and Hansen, 2015) of the form.

$$\dot{\epsilon} = A\tau^n \exp\left(-\frac{E + PV}{RT}\right) \quad (1)$$

where $\dot{\epsilon}$ represents strain rate (taken to be 10^{-14} s^{-1}), τ is deviatoric stress, P and T are pressure and temperature, respectively, R is the gas constant, and A , E , V , n are material parameters. We use a thermal model (Wade et al., 2017) for Archean and Phanerozoic lithosphere with mantle potential temperatures of 1650 °C and 1330 °C, respectively (Herzberg et al., 2010), and material parameters for olivine (Hirth and Kohlstedt, 2003), diabase (Mackwell et al., 1998), and quartzite (Hirth et al., 2001) for the structures illustrated below. Material parameters for dry and wet flow laws are utilised for the nominally anhydrous (NAn) and minimally hydrated (MHy) end-member cases.

4. Results

4.1. Petrology and density

Plots of density versus P - T conditions for each crustal lithology, age, and hydration state are shown in Fig. 3. Plots showing evolving

phase proportions during metamorphism are given in Supplementary Data, Figs. S1–S3. If subducted UCC is minimally hydrated with aqueous fluid – as suggested by field investigation (Deming, 1994) – basaltic intrusions of all ages transform to eclogite (Supplementary Data, Fig. S1) and become denser than pyrolite (Supplementary Data, Fig. S3) at 2.2–2.3 GPa and 600–640 °C (Fig. 3a). Mafic Archean UCC follows a similar evolution during descent, becoming denser than surrounding mantle at ~2.4 GPa (Fig. 3a); equivalent to ~75 km depth within the Earth and before the HP–UHP transition is crossed. Minimally hydrated granodioritic Phanerozoic and Proterozoic UCC contains jadeitic clinopyroxene, garnet, muscovite (phengite), and quartz/coesite at HP/UHP conditions, with or without rutile and glaucophane (Supplementary Data, Fig. S1). The calculated bulk-rock densities of these granodioritic compositions (2.9–3.2 g/cm³) always show positive buoyancy compared to the upper mantle (3.35 g/cm³; Fig. 3a). A composite orogenic terrane with a generous UCC:basalt volume ratio of 90:10 would reach a point-of-no-return of $P \sim 2.3$ GPa during the Archean (Fig. 3b), whereas more silica-rich Proterozoic and Phanerozoic crust remains positively buoyant up to at least ~3.5 GPa.

Calculated P - T -density profiles for nominally anhydrous lithologies metamorphosed along this geotherm (Fig. 3c) are different to results obtained assuming fluid saturation. All mafic crustal components – including bulk Archean UCC – transform to eclogite (Supplementary Data, Fig. S2) and show densities of 3.45–3.55 g/cm³ (Fig. 3c), making them negatively buoyant compared to pyrolite (Supplementary Data, Fig. S3). Intermediate Proterozoic and Phanerozoic UCC transforms to garnet-, kyanite-, and jadeite-

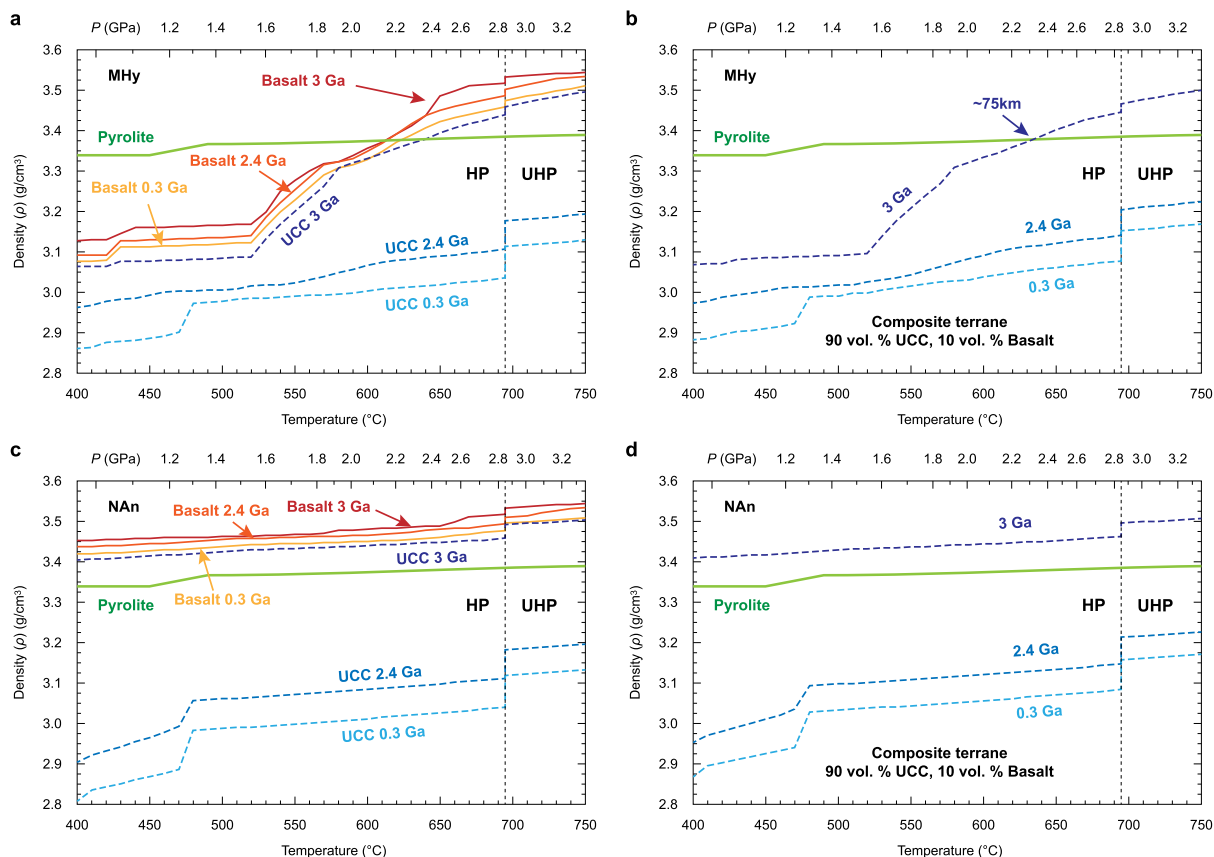


Fig. 3. Calculated density profiles along a typical subduction zone geotherm. Values for (a) minimally hydrated (MHy) continental crust and basalt and (b) composite terrane with volume proportions of these lithologies in the ratio 90:10, respectively, during metamorphism along an average subduction zone pressure–temperature (P – T) path. (c–d) As for parts a–b, but for nominally anhydrous (NAn) equivalents of each lithology.

bearing quartzofeldspathic gneiss during subduction (Supplementary Data, Fig. S2), which have a bulk density of 2.8–3.0 g/cm³ at P less than 1.2 GPa and 3.0–3.1 g/cm³ at the HP–UHP transition (Fig. 3c). These younger UCC components thus never achieve negative buoyancy within the limits of this model (P ~3.5 GPa) and may be readily exhumed if they can separate from the remainder of the sinking slab. A plot of bulk-terrane density for nominally anhydrous crustal components (Fig. 3d) shows that an Archean UCC that is mafic in composition always remains negatively buoyant compared to pyrolite. By contrast, both Proterozoic and Phanerozoic terranes have lower densities (~2.9–3.2 g/cm³) than surrounding mantle, akin to model results for minimal fluid saturation (Fig. 3b).

4.2. Sensitivity analysis

Checks on the validity of our petrological modeling results were performed by applying a Monte Carlo sensitivity analysis to the error in proportions of ultramafic (komatiite), mafic (greenstone), and felsic (TTG gneiss) components reported by Chen et al. (2020) for Mesoarchean UCC. These ranges were: 0–36 vol% (komatiite), 64–75 vol% (greenstone), and 0–25 vol% (TTG). We applied the Monte Carlo randomization procedure outlined by Palin et al. (2016) to generate 500 new estimations of the bulk Archean UCC composition. These spread mostly between the basalt and basaltic andesite fields on a conventional total alkali–silica (TAS) diagram (Supplementary Data, Fig. S4), with some positioned in the picobasalt, tephrite, and andesite fields. This analysis was applied to both anhydrous and minimally hydrated scenarios, as

described in the Methods section of the main manuscript. This procedure was not performed for felsic Proterozoic or Phanerozoic UCC, given the lower uncertainty of its composition and its strong negative buoyancy during subduction, as shown in Fig. 3. For the Archean UCC, eight discrete pressure–temperature (P – T) points were considered along the modelled path: 400 °C and 0.95 GPa, 450 °C and 1.16 GPa, 500 °C and 1.42 GPa, 550 °C and 1.72 GPa, 600 °C and 2.07 GPa, 650 °C and 2.46 GPa, 700 °C and 2.90 GPa, and 750 °C and 3.38 GPa.

Box and whisker plots (Fig. 4) for each of these P – T conditions demonstrate that crustal composition determined by Chen et al. (2020) using a komatiite–basalt–felsic rock ratio of 20:69:11 (Supplementary Data, Table S1) is representative of the total range as defined by their calculated errors, showing densities correlating more or less with the 50th percentile of the randomized set in each case. The calculated ‘point of no return’ for minimally hydrated Archean UCC discussed in the main manuscript, which occurs at ~2.3 GPa (Fig. 3), is reproduced by this sensitivity analysis (cf. Fig. 4). At slightly lower pressure, between 0% and 28% of all randomized bulk compositions exhibit negative buoyancy, although above 2.4 GPa, between 73% and 92% are denser than surrounding mantle pyrolite. For anhydrous equivalents, few randomized examples retain positive buoyancy compared to mantle pyrolite: from 22% to 33% below the quartz–coesite transition, and less than 19% above the transition. These data suggest that while some highly felsic crust may have the potential to be exhumed from Archean subduction zones without the help of external forcing, and in doing so may bias the rock record, this is not expected to be the norm.

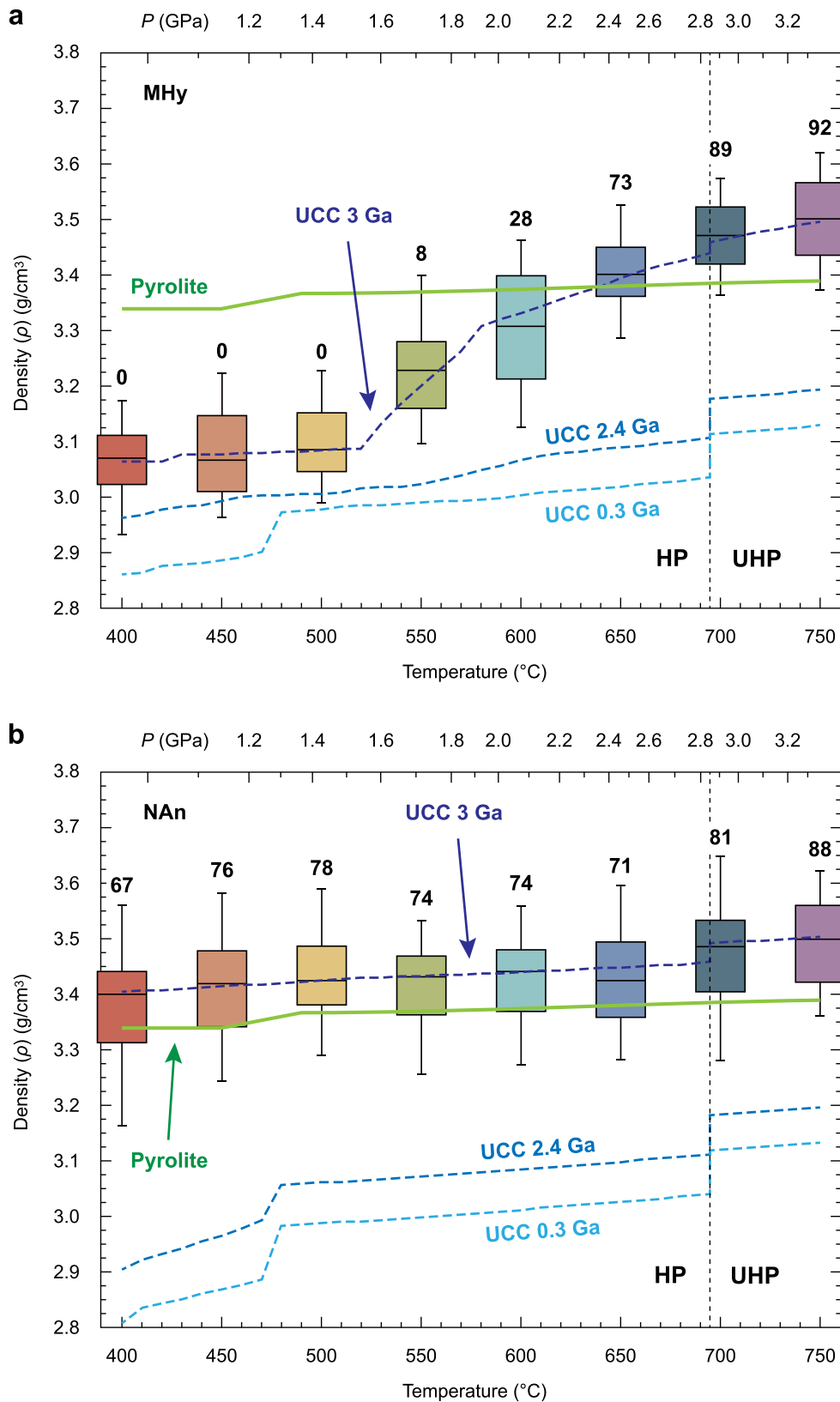


Fig. 4. Results of sensitivity analysis for the density of Archean (3 Ga) UCC during subduction. Density distributions are shown as box and whisker plots and consider 500 randomized bulk compositions determined at eight pressure–temperature (P – T) conditions. The upper and lower limits of each box are the 75th and 25th percentiles, respectively, the 50th percentile is the line within the box, and the whiskers represent the 5th and 95th percentiles. Numbers above each box show the percentage of data points for that P – T condition that have a density greater than surrounding pyrolite. All other annotations are taken from Fig. 3.

4.3. Isostatic balance

At the length scales of the continents, flexural effects may safely be neglected (Watts, 2001; Watts and Moore, 2017) and we model isostasy using a vertical balance, incorporating aspects of Airy (Airy, 1855) and Pratt (Pratt, 1859) isostasy. The pressure at the depth of compensation, D_c (Fig. 5) beneath oceanic lithosphere is given by:

$$P_o = [(\rho_w - \rho_m)h_o + (\rho_o - \rho_m)T_o + D_c\rho_m]g \quad (2)$$

and that for continental lithosphere in the Phanerozoic:

$$P_c = [\rho_c h_c + (\rho_c - \rho_m)(T_c - h_c) + D_c\rho_m]g \quad (3)$$

where ρ = density; w = water; o = oceanic lithosphere; m = asthenospheric mantle; c = Phanerozoic continental crust; h_o = water depth, h_c = topographic expression of the continents; T_o and T_c = thickness of the oceanic and continental crust respectively; and g = acceleration due to gravity. As the pressure will be equal at the depth of compensation, we can equate these two expressions and rearrange to solve for the average topographic expression of the continents, h_c :

$$h_c = \frac{\rho_m - \rho_c}{\rho_m} T_c - \frac{\rho_m - \rho_w}{\rho_m} h_o - \frac{\rho_m - \rho_o}{\rho_m} T_o \quad (4)$$

For typical values (Supplementary Data, Table S2) of Phanerozoic crust we retrieve values close to that of average modern continental topography (900 m) and adjusting the crustal thickness by 800 m produces an exact match. We then apply this model to Archean crustal values (Supplementary Data, Table S2), and replace the continental density ρ_c with:

$$\rho_{cA} = (1 - \lambda)\rho_c + \lambda\rho_o \quad (5)$$

with ρ_{cA} = density of Archean crust, and λ represents the basalt volume fraction in Archean continental crust. However, we retrieve a negative value (−1.2 km) for the average topography, indicating the continents were submerged. This violates our assumption that the continents were above the ocean surface and requires two modifications to the model: firstly, the water would represent an additional load in the isostatic balance calculation, and secondly, redistributing the volume of water across the whole planet would reduce the average water depth (h_o) over oceanic crust. Accounting for the redistribution of water and reversing the polarity of h_c as it now represents water depth above the continents gives

$$h_{oA} = h_o - \frac{3}{7}h_{cA} \quad (6)$$

with h_{oA} the water depth over Archean oceanic crust and h_{cA} the water depth over Archean continental crust. Here, we have assumed here that the volume of water present on the Earth during the Archean was no less than it is in the present day, as any additional volume would serve only to increase the water depth uniformly everywhere. Hence, Eq. (4) can be reframed as:

$$h_{cA} = \frac{7}{10} \left(h_o + \frac{\rho_m - \rho_o}{\rho_m - \rho_w} T_o - \frac{\rho_m - \rho_{cA}}{\rho_m - \rho_w} T_c \right) \quad (7)$$

and h_{cA} is interpreted as a lower bound on Archean water depth above the continents. When applied to Archean parameters (Supplementary Data, Table S2) we retrieve an average water depth over the continents of 1.3 km and a reduction in water depth over the oceans of 600 m relative to present day values.

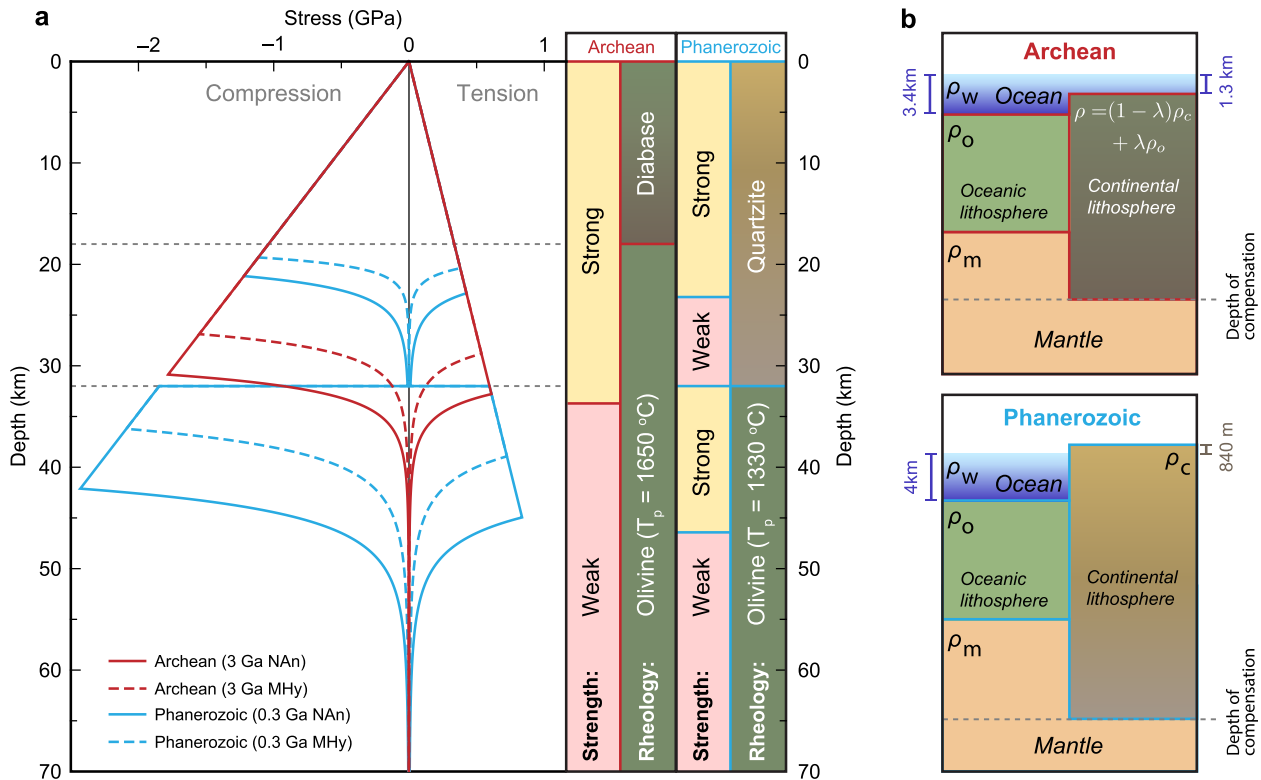


Fig. 5. Rheological and hypsometric implications of changes in continental crust composition. (a) Yield strength envelope (YSE) for Archean (red) and Phanerozoic (blue) lithosphere under nominally anhydrous (NAN, solid lines) and minimally hydrated (MHY, dashed lines) conditions. The relative strength of the lithosphere and rheology employed to generate the YSE are shown for reference. T_p = mantle potential temperature. (b) Schematic cross sections through Archean and Phanerozoic lithosphere demonstrating changes in hypsometry under isostatic equilibrium. ρ = density; w = water; o = oceanic lithosphere; m = asthenospheric mantle; c = Phanerozoic continental lithosphere; λ = basalt fraction in Archean continental crust.

5. Discussion

The age of onset of plate tectonics on Earth is strongly debated (Palin and Santosh, 2020), but relies fundamentally on identifying evidence for subduction having operated at different points in time. Many reliable indicators of subduction are petrological, such as blueschists, which only form along cold geothermal gradients (Palin and White, 2016); however, no blueschists occur in the geological record before c. 0.8 Ga (Maruyama et al., 1996). UHP metamorphism is also diagnostic of transporting crustal materials into the mantle (Gilotti, 2013). The oldest UHP eclogite on Earth formed at a similar time (c. 0.6 Ga) to the oldest blueschists, which has spawned arguments for a very recent onset of plate tectonics (Stern, 2005). Nonetheless, older HP eclogite in orogenic terranes occur as far back in the rock record as c. 2.09 Ga (Liou et al., 2009) and provides clear evidence for convergent margin processes during the Proterozoic.

Calculated densities for different continental terranes in this work (Fig. 3b, d) show that the reported highly basic composition of Archean UCC would have prohibited buoyancy-driven exhumation once UHP conditions were reached. The results of Monte Carlo sensitivity analysis support these data, with ~90% of randomised Archean UCC compositions showing the same shift from positive to negative buoyancy during descent before the HP-UHP transition is reached (Fig. 4). While we have utilized a typical geotherm for Phanerozoic-Proterozoic subduction zones (cf. Penniston-Dorland et al., 2015), we note that the proposition that Archean subduction zone slab-top geotherms were higher than the Phanerozoic acts to further support our interpretations. If subduction occurred along an elevated geotherm, the intercept of the geotherm and the HP-UHP transition would shift to higher pressures, given the positive (albeit shallow) dP/dT slope of the quartz-coesite transition. Thus, as eclogitization of all mafic rocks considered in this study occurs at a relatively consistent pressure of 2.3 GPa (cf. total proportion of garnet plus omphacite >75 vol%; Supplementary Data, Fig. S2), the point of no return would be reached for each terrane at a similar depth within the Earth, even if the geothermal gradient is elevated. This would still prohibit exhumation driven by buoyancy alone.

While we consider subduction as the transport mechanism, as many lines of evidence support its operation during the Archean (Shirey and Richardson, 2011), our results notably hold true even if transport into the mantle occurred via dripping or delamination of lower crust in a stagnant lid geodynamic regime (Piccolo et al., 2020). Metamorphic phase changes in low- and high-MgO Archean metabasalt experiencing 'sagduction'-type vertical transport into the mantle shows that eclogite-facies assemblages acquire negative buoyancy before the HP-UHP transition is reached (Wade et al., 2017). The paucity of felsic material at lower crustal levels (Rudnick and Gao, 2003; Fig. 2) further reduces the likelihood of these drips returning to the surface, unless driven by external forces. For subduction of a thinned continental margin immediately before collisional orogenesis, akin to formation of UHP eclogites in the Himalayan Range (St-Onge et al., 2013), we also note that our modelling focuses on the density of the UCC only, not the entire subducted slab. Nonetheless, field-based investigations and numerical modelling studies show that formation of UHP orogenic eclogite must involve whole-scale detachment of the continental terrane from the subducting mantle lithosphere due to localized strain weakening/grain size reduction, hydration, or melting (Agard et al., 2009; Warren et al., 2008). If the proto-exhumed terrane cannot mechanically detach from the downgoing root, the relative density contrast between UCC and pyrolyte (Fig. 3) becomes irrelevant, as total slab density will always exceed that of surrounding mantle. This confirms the importance of secular

compositional variation when interpreting changes in geodynamic processes through time (Weller and St-Onge, 2017), as the absence of (U)HP eclogite in Archean terranes is often alternatively attributed to overprinting following exhumation.

The Archean continental crust being more mafic than previously assumed has several broader implications for early Earth tectonics and continental hypsometry. Geodynamic models of the early Earth often assume continental crust to be broadly felsic and employ wet quartzite flow laws (Sizova et al., 2010); however, if volumetrically dominated by basalt (Chen et al., 2020 and others), a diabase flow law would be more appropriate. Further, when considering secular changes in both maficity and mantle potential temperature (Herzberg et al., 2010), the material strength of the Archean continents is markedly different to Phanerozoic equivalents. Calculated yield strength envelopes (Watts, 2001) reveal (Fig. 5a) that Archean continental crust is contiguous in strength, exhibiting a "crème brûlée" type of behaviour, as opposed to the Phanerozoic "jelly sandwich" model with a weak lower crust (Bürgmann and Dresen, 2008). Indeed, its mechanical properties more closely resemble those of modern oceanic crust than modern continents, with this relationship holding true for both nominally anhydrous and minimally fluid saturated end-member scenarios (Fig. 5a).

Models for vertical transport of lower crustal continental material into the mantle are characterised by two end members (Beall et al., 2017): short-wavelength drips (e.g. Rayleigh-Taylor instabilities) or longer-wavelength 'peels' (e.g. delamination). A prerequisite for delamination is the presence of a weak layer at the point of separation, thus allowing the lower continental crust to rheologically separate into contiguous layers. However, as the calculated yield strength envelope (Fig. 5a) for a mafic Archean continental crust does not exhibit a pronounced weak layer, unlike Phanerozoic continental crust, this implies that the primary mechanism for recycling of continental material into the mantle was dripping, in agreement with geodynamical models (Gerya, 2014). Finally, the above-average density (~2.87 g/cm³) and reduced thickness of Archean continents compared to Phanerozoic continents (Fig. 2) lowers the average isostatic elevation of the former by around 2.2 km relative to that of the present day (Fig. 5b; Lamb et al., 2020). This implies that the early Earth was likely covered by a global ocean with an average depth over the continental surface of ~1.3 km, in agreement with recent isotopic data (Johnson and Wing, 2020). It then follows that the emergence of a continental freeboard was itself driven by the secular chemical evolution of Earth's continental crust.

The transition to more felsic continental crust between the Archean and the Proterozoic (Figs. 1–2), and the resulting change in isostatic balance, supports models of changing freeboard over time that imply a Late Archean (c. 2.5 Ga) emergence of the continents (Flament et al., 2008), which has been associated with the Great Oxygenation Event soon afterwards (Gumsley et al., 2017). Furthermore, the presence or otherwise of sub-aerial land is, potentially, a key component in the origin of life. Origin scenarios that invoke the initiation of life at serpentinising hydrothermal vents have been contested on a number of grounds, not least the elevated temperatures of vents aqueous environment are unfavourable to the chemical kinetics and stability of peptide bonds (Rodriguez-Garcia et al., 2015). To overcome these limitations, alternative scenarios utilise the presence of sub-aerial land to provide both the raw chemical constituents and temporally wet surfaces (Powner et al., 2009). Cycling between wet and dry environments may promote the formation of vesicles and cell-like structures (Deamer and Barchfeld, 1982), whilst also limiting the deleterious effects of dilute aqueous environments. The appearance of life in the deep Archaeon (Arndt and Nisbet, 2012) and

the likely absence of sub-aerial land are then in conflict with a terrestrial origin for life. Hence, the secular abundance of surface water and crust play a key role not just in our understanding of the early Earth's surface environment, but also in the story of life itself.

6. Conclusions

Ultrahigh pressure (UHP) eclogite is absent from the geological record prior to c. 0.6 Ga, and high-pressure eclogite associated with orogenesis is absent from rocks older than c. 2.1 Ga; however, subduction-related geological imprints have been widely documented in many Archean terranes, with some researchers proposing that plate tectonics had begun on Earth during the Hadean (c. 4.2 Ga). The absence of (U)HP orogenic eclogite from Archean terranes has hitherto been ascribed to a lack of preservation, or non-formation from researchers who argue that subduction had not operated at all during this period. Our petrological modelling examined the changing petrophysical characteristics of continental crust through time, which recent geochemical proxies have shown was notably more mafic in the Archean than previously thought. Our calculations show that mafic Archean continents would have transformed to eclogitic assemblages and acquired negative buoyancy compared to surrounding pyrolite-like mantle *before* the HP-UHP transition was reached, thus inhibiting their return to the surface via buoyancy. By contrast, more silicic Proterozoic and Phanerozoic continental crust could have retained a positive bulk buoyancy to greater depths within the Earth – after passing the HP-UHP transition – and so could be readily exhumed, if able to mechanically detach from the remainder of the descending slab. This secular change in continental crust thus has had significant imprints on the metamorphic/tectonic rock record.

This documented change in continental crust composition has additional critical effects on our understanding of the early Earth. To be in isostatic equilibrium, a more mafic Archean continental crust would have been thinner and more low-lying than felsic or intermediate Phanerozoic or Proterozoic equivalents. Isostatic balance calculations thus imply that the Archean continents were likely submerged beneath an ocean over 1 km deep, impinging on hypotheses for the emergence of life that rely on subaerial land at this time. Further, the more mafic mineralogy of Archean continents would have led them to have yield strength envelopes that more closely resemble modern-day oceanic crust, than modern-day continental crust. The absence of a mid-crustal weak layer in calculated yield strength envelopes implies that the primary mechanism for recycling of continental material into the mantle on the early Earth was dripping – not delamination – in agreement with many geodynamical models.

Declaration of Competing Interest

The authors declare that they have no known competing financial interests or personal relationships that could have appeared to influence the work reported in this paper.

Acknowledgements

The authors are grateful for comments on earlier version of this work by Clare Warren, Alan Hastie, and Daniel Wiemer, and formal comments on this most recent version by two anonymous reviewers. JDPM acknowledges support from Marsden grant 14-VUW-085, Royal Society of New Zealand. Codes for reproducing the isostatic balance calculation and yield strength envelopes may be found at www.jamesdpmoore.com.

Appendix A. Supplementary data

Supplementary data to this article can be found online at <https://doi.org/10.1016/j.gsf.2021.101225>.

References

- Agard, P., Yamato, P., Jolivet, L., Burov, E., 2009. Exhumation of oceanic blueschists and eclogites in subduction zones: timing and mechanisms. *Earth Science Reviews* 92, 53–79.
- Airy, G.B., 1855. On the computation of the effect of the attraction of mountain masses, as disturbing the apparent astronomical latitude of stations in geodetic surveys. *Philosophical Transactions of the Royal Society* 145, 101–104.
- Arndt, N.T., Nisbet, E.G., 2012. Processes on the young earth and the habitats of early life. *Annual Review of Earth and Planetary Sciences* 40, 521–549.
- Beall, A.P., Moresi, L., Stern, T., 2017. Dripping or delamination? A range of mechanisms for removing the lower crust or lithosphere. *Geophysical Journal International* 210, 671–692.
- Bialas, R.W., Funicello, F., Faccenna, C., 2011. Subduction and exhumation of continental crust: Insights from laboratory models. *Geophysical Journal International* 184, 43–64.
- Bolhar, R., Kamber, B.S., Moorbath, S., Whitehouse, M., Collerson, K.D., 2005. Chemical characterization of Earth's most ancient clastic metasediments from the Isua Greenstone belt, southern west Greenland. *Geochimica et Cosmochimica Acta* 69, 1555–1573.
- Boutelier, D., Chemenda, A., Jorand, C., 2004. Continental subduction and exhumation of high-pressure rocks: insights from thermo-mechanical laboratory modelling. *Earth and Planetary Science Letters* 222, 209–216.
- Bürgmann, R., Dresen, G., 2008. Rheology of the lower crust and upper mantle: Evidence from rock mechanics, geodesy, and field observations. *Annual Review of Earth and Planetary Sciences* 36, 531–567.
- Byerlee, J., 1978. Friction of rocks. *Pure and Applied Geophysics* 116, 615–626.
- Chapman, T., Clarke, G.L., Daczko, N.R., 2019. The role of buoyancy in the fate of ultrahigh pressure eclogite. *Scientific Reports* 9, 1–9.
- Chen, K., Rudnick, R.L., Wang, Z., Tang, M., Gaschnig, R.M., Zou, Z., He, T., Hu, Z., Liu, Y., 2020. How mafic was the Archean upper continental crust? Insights from Cu and Ag in ancient glacial diamictites. *Geochimica et Cosmochimica Acta* 278, 16–29.
- Coleman, R.G., Lee, D.E., Beatty, L.B., Brannock, W.W., 1965. Eclogites and eclogites: their differences and similarities. *Geological Society of America Bulletin* 76, 483–508.
- Condie, K.C., 1993. Chemical composition and evolution of the upper continental crust: contrasting results from surface samples and shales. *Chemical Geology* 104, 1–37.
- Condie, K.C., Aster, R.C., Van Hunen, J., 2016. A great thermal divergence in the mantle beginning 2.5 Ga: Geochemical constraints from greenstone basalts and komatiites. *Geoscience Frontiers* 7, 543–553.
- De Capitani, C., Petrakakis, K., 2010. The computation of equilibrium assemblage diagrams with ThermoCalc software. *American Mineralogist* 95, 1006–1016.
- Deamer, D.W., Barchfeld, G.L., 1982. Encapsulation of macromolecules by lipid vesicles under simulated prebiotic conditions. *Journal of Molecular Evolution* 18, 203–206.
- Deming, D., 1994. Fluid flow and heat transport in the upper continental crust. *Geological Society London Special Publications* 78, 27–42.
- Dhuime, B., Wuestefeld, A., Hawkesworth, C.J., 2015. Emergence of modern continental crust about 3 billion years ago. *Nature Geosciences* 8, 552–556.
- Flament, N., Coltice, N., Rey, P.F., 2008. A case for Late Archean continental emergence from thermal evolution models and hypsometry. *Earth and Planetary Science Letters* 275, 326–336.
- Forshaw, J.B., Waters, D.J., Pattison, D.R., Palin, R.M., Gopon, P., 2019. A comparison of observed and thermodynamically predicted phase equilibria and mineral compositions in mafic granulites. *Journal of Metamorphic Geology* 37, 153–179.
- Gerya, T., 2014. Precambrian geodynamics: Concepts and models. *Gondwana Research* 25, 442–463.
- Gilotti, J.A., 2013. The realm of ultrahigh-pressure metamorphism. *Elements* 9, 255–260.
- Greber, N.D., Dauphas, N., Bekker, A., Ptáček, M.P., Bindeman, I.N., Hofmann, A., 2017. Titanium isotopic evidence for felsic crust and plate tectonics 3.5 billion years ago. *Science* 357, 1271–1274.
- Green, E.C.R., White, R.W., Diener, J.F.A., Powell, R., Holland, T.J.B., Palin, R.M., 2016. Activity–composition relations for the calculation of partial melting equilibria in metabasic rocks. *Journal of Metamorphic Geology* 34, 845–869.
- Gumsley, A.P., Chamberlain, K.R., Bleeker, W., Söderlund, U., de Kock, M.O., Larsson, E.R., Bekker, A., 2017. Timing and tempo of the Great Oxidation Event. *Proceedings of the National Academy of Sciences of the United States of America* 114, 1811–1816.
- Hacker, B.R., 2006. Pressures and temperatures of ultrahigh-pressure metamorphism: implications for UHP tectonics and H₂O in subducting slabs. *International Geology Review* 48, 1053–1066.
- Hatiy, R., 1822. *Traité de Minéralogie*. Bachelier et Huzar, Paris.
- Hawkesworth, C.J., Cawood, P.A., Dhuime, B., 2016. Tectonics and crustal evolution. *GSA Today* 9, 4–11.
- Hernández-Urbe, D., Palin, R.M., 2019. A revised petrological model for subducted oceanic crust: Insights from phase equilibrium modelling. *Journal of Metamorphic Geology* 37, 745–768.

- Herzberg, C., Condie, K., Korenaga, J., 2010. Thermal history of the Earth and its petrological expression. *Earth and Planetary Science Letters* 292, 79–88.
- Hirth, G., Kohlstedt, D., 2003. Rheology of the upper mantle and the mantle wedge: A view from the experimentalists. *Geophysical Monograph American Geophysical Union* 4, 1–24.
- Hirth, G., Teyssier, C., Dunlap, J., 2001. An evaluation of quartzite flow laws based on comparisons between experimentally and naturally deformed rocks. *International Journal of Earth Sciences* 90, 77–87.
- Holland, J.G., Lambert, R.S.T., 1972. Major element chemical composition of shields and the continental crust. *Geochimica et Cosmochimica Acta* 36, 673–683.
- Holland, T.J.B., Powell, R., 2003. Activity–composition relations for phases in petrological calculations: an asymmetric multicomponent formulation: *Contrib. Mineralogy and Petrology* 145, 492–501.
- Holland, T.J.B., Powell, R., 2011. An improved and extended internally consistent thermodynamic dataset for phases of petrological interest, involving a new equation of state for solids. *Journal of Metamorphic Geology* 29, 333–383.
- Jennings, E.S., Holland, T.J.B., 2015. A simple thermodynamic model for melting of peridotite in the system NCFMASOcr. *Journal of Petrology* 56, 869–892.
- Johnson, B.W., Wing, B.A., 2020. Limited Archean continental emergence reflected in an early Archean ^{18}O -enriched ocean. *Nature Geosciences* 13, 243–248.
- Kirby, S.H., Durham, W.B., Stern, L.A., 1991. Mantle phase changes and deep-earthquake faulting in subducting lithosphere. *Science* 252, 216–225.
- Kohlstedt, D.L., Hansen, L.N., 2015. Constitutive equations, rheological behavior, and viscosity of rocks. *Treatise on Geophysics (Second Edition)* 2 (2), 441–472.
- Korenaga, J., 2013. Initiation and evolution of plate tectonics on Earth: theories and observations. *Annual Review of Earth and Planetary Sciences* 41, 117–151.
- Lamb, S., Moore, J.D.P., Perez-Gussinyà, M., Stern, T., 2020. Global whole lithosphere isostasy: implications for surface elevations, strength and densities of the continental lithosphere. *Geochemistry, Geophysics, Geosystems* 21. <https://doi.org/10.1029/2020GC009150>.
- Le Losq, C., Berry, A.J., Kendrick, M.A., Neuville, D.R., O'Neill, H.S.C., 2019. Determination of the oxidation state of iron in Mid-Ocean Ridge basalt glasses by Raman spectroscopy. *American Mineralogist* 104, 1032–1042.
- Liou, J.G., Ernst, W.G., Zhang, R.Y., Tsujimori, T., Jahn, B.M., 2009. Ultrahigh-pressure minerals and metamorphic terranes – The view from China. *Journal of Asian Earth Sciences* 35, 199–231.
- Loose, D., Schenk, V., 2018. 2.09 Ga old eclogites in the Eburnian-Transamazonian orogen of southern Cameroon: Significance for Palaeoproterozoic plate tectonics. *Precambrian Research* 304, 1–11.
- Mackwell, S.J., Zimmerman, M.E., Kohlstedt, D.L., 1998. High-temperature deformation of dry diabase with application to tectonics on Venus. *Journal of Geophysical Research* 103, 975–984.
- Martin, B., Moyen, J.F., 2002. Secular changes in tonalite-trondhjemite-granodiorite composition as markers of the progressive cooling of Earth. *Geology* 30, 319–322.
- Maruyama, S., Liou, J.G., Terabayashi, M., 1996. Blueschists and eclogites of the world and their exhumation. *International Geology Review* 38, 485–594.
- Palin, R.M., White, R.W., 2016. Emergence of blueschists on Earth linked to secular changes in oceanic crust composition. *Nature Geosciences* 9, 60–64.
- Palin, R.M., Santosh, M., 2020. Plate tectonics: What, where, why, and when?. *Gondwana Research* 100. <https://doi.org/10.1016/j.gr.2020.11.001>.
- Palin, R.M., Weller, O.M., Waters, D.J., Dyck, B., 2016. Quantifying geological uncertainty in metamorphic phase equilibria modelling; a Monte Carlo assessment and implications for tectonic interpretations. *Geoscience Frontiers* 7, 591–607.
- Palin, R.M., Reuber, G.S., White, R.W., Kaus, B.J., Weller, O.M., 2017. Subduction metamorphism in the Himalayan ultrahigh-pressure Tso Moriri massif: an integrated geodynamic and petrological modelling approach. *Earth and Planetary Science Letters* 467, 108–119.
- Palin, R.M., Santosh, M., Cao, W., Li, S.S., Hernández-Urbe, D., Parsons, A., 2020. Secular change and the onset of plate tectonics on Earth. *Earth Science Reviews* 207, 103172.
- Penniston-Dorland, S.C., Kohn, M.J., Manning, C.E., 2015. The global range of subduction zone thermal structures from exhumed blueschists and eclogites: Rocks are hotter than models. *Earth and Planetary Science Letters* 428, 243–254.
- Piccolo, A., Kaus, B.J., White, R.W., Palin, R.M., Reuber, G.S., 2020. Plume–lid interactions during the Archean and implications for the generation of early continental terranes. *Gondwana Research* 88, 150–168.
- Powney, M.W., Gerland, B., Sutherland, J.D., 2009. Synthesis of activated pyrimidine ribonucleotides in prebiotically plausible conditions. *Nature* 459, 239–242.
- Pratt, J.H., 1859. On the deflection of the plumb-line in India, caused by the attraction of the Himalaya mountains and of the elevated regions beyond; and its modification by the compensating effect of a deficiency of matter below the mountain mass. *Philosophical Transactions of the Royal Society* 149, 745–778.
- Ringwood, A.E., 1975 *Composition and Petrology of the Earth's Mantle*. MacGraw-Hill, 618.
- Rodríguez-García, M., Surman, A.J., Cooper, G.J., Suárez-Marina, I., Hosni, Z., Lee, M. P., Cronin, L., 2015. Formation of oligopeptides in high yield under simple programmable conditions. *Nature Communications* 6, 8385.
- Rudnick, R.L., Gao, S., 2003. Composition of the continental crust: The crust. 3, 1–64.
- Shirey, S.B., Richardson, S.H., 2011. Start of the Wilson cycle at 3 Ga shown by diamonds from subcontinental mantle. *Science* 333, 434–436.
- Sizova, E., Gerya, T., Brown, M., Perchuk, L.L., 2010. Subduction styles in the Precambrian: Insight from numerical experiments. *Lithos* 116, 209–229.
- Stagno, V., Ojwang, D.O., McCammon, C.A., Frost, D.J., 2013. The oxidation state of the mantle and the extraction of carbon from Earth's interior. *Nature* 493, 84–88.
- Staudigel, H., 2003. Hydrothermal alteration processes in the oceanic crust: *Treat. Geochemistry* 3, 659–681.
- Stern, R.J., 2005. Evidence from ophiolites, blueschists, and ultrahigh-pressure metamorphic terranes that the modern episode of subduction tectonics began in Neoproterozoic time. *Geology* 33, 557–560.
- St-Onge, M.R., Rayner, N., Palin, R.M., Searle, M.P., Waters, D.J., 2013. Integrated pressure–temperature–time constraints for the Tso Moriri dome (Northwest India): implications for the burial and exhumation path of UHP units in the western Himalaya. *Journal of Metamorphic Geology* 31, 469–504.
- Tang, M., Chen, K., Rudnick, R.L., 2016. Archean upper crust transition from mafic to felsic marks the onset of plate tectonics. *Science* 351, 372–375.
- Taylor, S.R., McLennan, S.M., 1995. The geochemical evolution of the continental crust. *Reviews of Geophysics* 33, 241–265.
- Wade, J., Dyck, B., Palin, R.M., Moore, J.D., Smye, A.J., 2017. The divergent fates of primitive hydrospheric water on Earth and Mars. *Nature* 552, 391–394.
- Warren, C.J., 2013. Exhumation of (ultra)-high-pressure terranes: concepts and mechanisms. *Solid Earth* 4, 75–92.
- Warren, C.J., Beaumont, C., Jamieson, R.A., 2008. Formation and exhumation of ultra-high-pressure rocks during continental collision: Role of detachment in the subduction channel. *Geochemistry, Geophysics, Geosystems*, 9(4), Q04019, doi:10.1029/2007GC001839.
- Watts, A.B., 2001. *Isostasy and Flexure of the Lithosphere*. Cambridge University Press, Cambridge, 458p.
- Watts, A.B., Moore, J.D., 2017. Flexural isostasy: Constraints from gravity and topography power spectra. *Journal of Geophysical Research: Solid Earth* 122, 8417–8430.
- Weller, O.M., St-Onge, M.R., 2017. Record of modern-style plate tectonics in the Palaeoproterozoic Trans-Hudson orogen. *Nature Geosciences* 10, 305–311.
- Weller, O.M., Copley, A., Miller, W.G.R., Palin, R.M., Dyck, B., 2019. The relationship between mantle potential temperature and oceanic lithosphere buoyancy. *Earth and Planetary Science Letters* 518, 86–99.
- White, R.W., Powell, R., Holland, T.J.B., Green, E.C.R., 2014. New mineral activity–composition relations for thermodynamic calculations in metapelitic systems. *Journal of Metamorphic Geology* 32, 261–286.
- White, R.W., Powell, R., Holland, T.J.B., Worley, B.A., 2000. The effect of TiO_2 and Fe_2O_3 on metapelitic assemblages at greenschist and amphibolite facies conditions: mineral equilibria calculations in the system K_2O – FeO – MgO – Al_2O_3 – SiO_2 – H_2O – TiO_2 – Fe_2O_3 . *Journal of Metamorphic Geology* 18, 497–511.
- Zheng, Y., Zhao, Z., Chen, Y., 2013. Continental subduction channel processes: Plate interface interaction during continental collision. *Chinese Science Bulletin* 58, 4371–4377.